Journal of ELECTRONIC MATERIALS, Vol. 40, No. 10, 2011
DOI: 10.1007/s11664-011-1706-x

On the Role of Boron in CdTe and CdZnTe Crystals

M. PAVESI,[1,2] L. MARCHINI,[1] M. ZHA,[1] A. ZAPPETTINI,[1,3] M. ZANICHELLI,[1,2] and M. MANFREDI[2]

1.—IMEM-CNR, Viale G.P. Usberti 37/A, 43124 Parma, Italy. 2.—Department of Physics, University of Parma, Viale G.P. Usberti 7/A, 43124 Parma, Italy. 3.—e-mail: zapp@imem.cnr.it

It is well known that group III elements act as donors if they play a substitutional role at the metallic site in II-tellurides; nevertheless, several studies report both on the creation of complexes with vacancies, named A-centers, and on the involvement in self-compensation mechanisms, especially for indium. The boron concentration in II-tellurides is negligible, and its contribution to transport mechanisms has not been studied yet. For the last few years the authors have been developing a new technique to grow CdZnTe by the vertical Bridgman technique, taking advantage of encapsulation by means of boron oxide. In this way, crystals characterized by large single grains, low etch pit density, and high resistivity have been obtained. Recently, x-ray detectors with state-of-the-art performance have been produced from such crystals. Boron contamination, as a consequence of this growth method, is quite low but at least one order of magnitude above values obtained with other growth techniques. Besides being a low-cost technique which is also suitable for large-scale mass production, the encapsulated vertical Bridgman technique is quite useful to prevent dislocations, grain boundaries, and stacking faults; for these reasons, careful characterization was performed to understand the effect of boron both on the electrical properties and on the spectroscopic performance of the final crystals. Our characterization is mainly based on low-temperature photoluminescence in addition to electrical current–voltage measurements, photostimulated current, and x-ray spectroscopy. The results indicate that boron behaves like other group III elements; in fact, boron forms a complex that does not affect the good performance of our x-ray detectors, even if it shows some properties which are typical of A-centers.

Key words: CdTe, CdZnTe, x-ray detectors, defects, impurities, photoluminescence

INTRODUCTION

Cadmium zinc telluride is well suited to application in energy-dispersive spectroscopy of high-energy radiation, such as x-rays and gamma-rays, due to its good spectral resolution and high counting efficiency even at room temperature. Great efforts have been made to improve its crystal quality and monocrystalline material yield. A large number of growth techniques have been successfully employed.[1] Among them, the Bridgman method represents a low-cost and easy way to achieve mass production of CdTe and CdZnTe, even if the use of a crucible is inadvisable because it can affect the quality of the final crystal.

The interaction between crystal and crucible in CdZnTe (CZT) growth seems to be the main reason for spurious nucleation.[2,3] It is well known that, the wetter the crucible walls get, the stickier the final solid is. For this reason, quartz or graphite are not recommended, the latter also for its carbon contamination of the melt. On the other hand, pyrolitic boron nitride demonstrates no chemical reactivity and the highest contact angle with molten GaAs,

(Received October 11, 2010; accepted June 20, 2011; published online July 15, 2011)

CdTe,[4] and CZT; unfortunately, this hexagonal material is very expensive and its anisotropic properties make it less attractive. Good-quality crystals have been obtained under dewetting conditions, which are only possible under microgravity or by applying a pressure difference between the melt and the solidifying crystal; however, technical problems associated with this technique prevent its use in large-scale production.

Twin and grain boundaries are one of the main causes of the poor electrical and spectroscopic features of CZT. In an effort to develop a procedure to grow ingots with high purity and large single grains, a new Bridgman configuration for growth of CZT crystals[5,6] was studied in our laboratories. In contrast to the standard vertical Bridgman technique, the crystal is grown in an open ampoule, melt decomposition being prevented by use of a boron oxide layer and an opportune counterpressure of inert gas.

In this geometry, there is no free volume above the melt, so that decomposition of the charge is avoided, no soldering procedures are necessary because the growth ampoule is open, and finally the growth process is completely safe, due to the fact that the crucible walls do not experience a pressure gradient.

A possible drawback is the chance of boron dioxide contaminating the charge.

All elements of groups I, III, IV, V, and VII act as dopants in CZT. The nature of the dopant, i.e., acceptor or donor, is determined by the structural position of the point defect, and in most cases, the electrical activity of these centers is very low.[1] As widely discussed in the literature, these point defects are frequently responsible for the self-compensation of material,[7] but their effects on the spectroscopic features of detectors have never been discussed.

Boron, as well as indium, can replace the cation, but boron is smaller and therefore could be interstitial or involved in aggregates with other point defects. Boron contamination was shown to be typically quite low[5] in our material. CdTe crystals grown by the Czochralski technique using boron oxide as an encapsulant showed *n*-type conduction, but the authors concluded that boron was not electrically active.[8] The same conclusion was reached after observing that samples grown under a boron oxide layer showed the same electrical behavior as samples grown by physical vapor transport without boron oxide.[9]

In spite of the very low concentration of boron in our crystals, we wanted to check if this new growth method could be useful for production of large quantities of spectroscopic material, and for this purpose, we investigated if this impurity can affect first the optical properties of the material, using the very sensitive technique of photoluminescence, and then the electrical and spectroscopic performance of detectors.

CZT crystals were grown by both the boron oxide encapsulated vertical Bridgman (EVB) technique and by the traditional vertical Bridgman (VB) technique in a closed ampoule. It is shown that a boron oxide layer fully encapsulates the crystal, thus preventing contact between the growing crystal and the crucible.

No appreciable changes in terms of current–voltage (*I–V*) measurements or x-ray spectroscopy were evidenced when comparing samples made using the different growth procedures. On the other hand, photocurrent (PC) measurements suggested an interaction between boron and the host lattice.

Photoluminescence (PL) is very sensitive to microscopic details, but no contribution, which might have been caused by the presence of boron, was observed, as a consequence of the high crystalline disorder in the CZT ternary alloy. For this reason, crystals of CdTe were grown by the encapsulated vertical Bridgman technique, and PL analysis showed, in this case, new features which are not ascribable to other impurities contained as traces inside the crystals. This result was related, for the first time, to the presence of boron and can be considered as due to an interaction of boron with other point defects.

EXPERIMENTAL PROCEDURES

The charge material was prepared from 7 N (Te, Cd) and 6 N (Zn) elements according to the process described elsewhere.[10] After synthesis, the charge was heat-treated at about 870°C to obtain a reproducible charge composition[11] and then charged into a quartz ampoule. The ampoule was closed only when the charge was not covered by a boron oxide pellet (water content 200 ppm, 99.9995% nominal purity). To obtain high-resistivity material, only CZT crystals were doped with indium in the range of 10^{17} atoms cm^{-3} to 10^{18} atoms cm^{-3}. The zinc content was 0.1 for all our crystals.

The furnace has three independent heating zones, and the growth chamber is pressurized to 5 atm to 10 atm to avoid charge decomposition. At the beginning of the growth procedure, the ampoule is kept in the upper part of the furnace, which is previously pressurized with inert gas. The temperature of the furnace is gradually increased until boron oxide starts softening at about 450°C. After the charge has melted, the ampoule is lowered at a speed of 1 mm h^{-1} to 2 mm h^{-1} and our crystal grows without use of a seed. The thermal gradient at the melt–crystal interface is about 10°C cm^{-1}.

Lastly, one of the main parameters affecting the detector quality of CdZnTe is the background impurity content. Table I presents glow discharge mass spectroscopy (GDMS) analysis of our EVB CZT crystals. Impurities with contents lower than the detection limit of the technique are not shown. It is interesting to observe that the impurity with the highest concentration is boron, which can be mainly

Table I. Background impurity content as determined by GDMS analysis in boron-encapsulated grown crystals of CZT

Element	Concentration (ppba)
B	800
C	20
N	23
O	340
Cr	10
Fe	210
Ga	43
In	8000

attributed to contamination by boron oxide. The contamination is about one order of magnitude lower than the concentration of the dopant (In $\sim 1 \times 10^{17}$ cm^{-3} in the final crystal) that we intentionally used to obtain high-resistivity CZT. It is worth considering the comparison with the boron content in VB crystals, where the content is too low to be detected; concentration of other impurities is similar to that found in EVB samples.

The concentration of oxygen is high as well, perhaps due to boron oxide itself. However, other possible sources of oxygen contamination could be the quartz ampoule, or the elements themselves, due to the fact that oxygen is usually not considered when computing total impurity content. Another impurity which is detectable at high concentration is iron. Unfortunately, although every precaution had been taken, we were not able to get rid of this contaminant, whose origin remains unclear. All other impurities had quite low concentrations.

Ingots of CZT grown by EVB and VB were cut into wafers of thickness of about 0.1 cm using a diamond-coated steel wire saw. To evaluate the dislocation density, Nakagawa etching was performed on some wafers that had been previously cut parallel to the (111) plane. The etch pit density (EPD) determined by counting the etch pits along the wafer radius is typically less than 10^4 cm^{-2}.

Samples of about 0.5 mm × 0.5 mm in size were prepared by mechanical polishing with abrasive paper and 0.05-μm particle size alumina suspension, then they were rinsed in methanol and chemically etched before contact deposition. Surfaces are chemically treated using a two-step procedure, first with a 2% bromine in methanol etching solution for 3 min followed by a mixed solution of 2% bromine in methanol, 20% lactic acid, and then with ethylene glycol for 2 min. After each etching, samples were rinsed in methanol. Surface oxidation was carried out with a NH_4F/H_2O_2 solution for 6 min at room temperature, thus ensuring the formation of a layer of about 70 nm, as shown by ellipsometric measurements.[12]

Samples for electrical characterization were subjected to evaporation of 750-Å-thick 0.3 cm × 0.3 cm square semitransparent gold contacts on the opposite sample surfaces, followed by thermal treatment at 80°C for 70 h in N_2 atmosphere. Photolithography with contact masks and lift-off processing were utilized to pattern the Au contacts. Samples were pasted onto a high-resistivity support using a bicomponent epoxy silver paste and bonded with Au wires. Zn content uniformity along the samples was checked by scanning electron microscopy (SEM) microanalysis.

PL spectra were recorded using an argon laser (515 nm) for excitation, and the signal was detected alternately with a silicon and an InGaAs photodiode. The samples were mounted inside a cryostat so that the temperature could be varied down to 6 K. The setup was provided with a scanning system that made it possible to map the homogeneity of the PL response over the sample. The signal was analyzed by means of a fast Fourier transform interferometer.

The experimental photocurrent apparatus consisted of a light source system (ORIEL mod. 66882), suitably screened and focused, with a 250-W quartz tungsten halogen lamp (~ 1 μW cm^{-2} nm^{-1} on the sample), a monochromator (CornerStone 130TM 1/8 m mod. 74000) covering the range of 200 nm to 1600 nm (wavelength resolution 3 nm), a chopper (Signal Recovery mod. 197) operating at 220 Hz, and a lock-in amplifier (EG&G PARK mod. 5209).

The chopped monochromatic light was focused onto a 3 mm × 3 mm area centered within the metal contact, as well as the sample operates as in the high-energy detector configuration. Besides, pair generation involves mainly a region of material where the electric field is almost uniform. The transparency of the gold contacts, in the energy range of interest, ensures that a sufficient percentage of the incident radiation reaches the sample surface. The spectral distribution of the beam illuminating the sample was measured using a Hamamatsu photonic multichannel analyzer (PMA-11), and a correction factor was introduced for all the measured spectra, taking into account the spectral distortion due to the gold contacts as measured for a reference gold layer of the same thickness deposited on quartz. The mean photon flux on the active surface of the CZT sample (i.e., below the metal contact) was estimated at around 10^{11} photons s^{-1} for an incident flux of 1 μW cm^{-2}. The output signal, collected as the voltage drop across a load resistance R (10 kΩ), was analyzed by the lock-in amplifier to reduce noise and to remove the dark current contribution.

PC spectra were acquired at fixed bias in the range of 200 nm to 1600 nm, and current–voltage (I–V) curves were measured without illumination or at fixed wavelength of incident photons by means of a source meter (Keithley 2400). From these latter curves, careful fitting with Many's equation[13] allows evaluation of the mobility–lifetime product $\mu\tau$ and the carrier surface recombination parameter s/μ for electron and holes. The sample thickness is

required, and the saturation current at high electric field is the third term given by the fitting.

Due to the choice of the contact geometry, the electric field was applied in the direction of incoming light, as in x-ray detectors operating under standard conditions. By convention, positive bias relates to the situation in which the anode is the illuminated electrode.

RESULTS AND DISCUSSION

Photoluminescence on CZT and CdTe

In CdTe and in CZT, creation of complexes between elements of group III (Ga, In) or group VII (F, Cl, Br, I) and V_{Cd} leading to radiative donor–acceptor pair (DAP) recombination, known as A-center band, was experimentally demonstrated. The role of these complexes and these dopants, acting as donors on II-sites or VI-sites for elements of group III or VII, respectively, in self-compensation mechanisms has also been discussed.[14]

Boron, as well as aluminum, is a light element of group III with empty *d*-shell, and its role as a dopant or contaminant has never been discussed before. Its small size could allow the formation of interstitials, as happens for Li, or substitutions (acceptors) at Cd sites; it is well known that lithium takes part in compensation only in the former case. The creation of DX-centers, which are characterized by a significant lattice relaxation, is unlikely for such a small atom as boron, unlike aluminum, gallium, and indium.[15] Besides, since boron belongs to group III, the creation of A-centers is a realistic hypothesis.

The new growth method using boron oxide encapsulation has potential for CZT production on a large scale only if boron contamination does not affect the high resistivity of the final device. For this reason, even if the boron concentration proved rather low in our crystals, one of our main concerns was to check its role as a defect and its contribution to the electrical properties of our material.

Low-temperature PL is a very sensitive technique to reveal the presence of defects and impurity complexes even at low concentration. The typical PL spectrum at 10 K for indium-doped CZT (zinc 10%) and grown with encapsulant (EVB) is shown in Fig. 1a in comparison with the spectrum of a sample grown without boron oxide (Fig 1b). The band-edge region is dominated by the neutral acceptor-bound excitonic line (A°-X) at 1.646 eV, related to a complex associated with Cd vacancies,[1] and the neutral donor-bound excitonic one (D°-X) at 1.658 eV, with similar intensities as expected in an almost intrinsic material. Due to the low effective mass of donors, it is not possible to observe the presence of isolated boron donor within the D°-X line.

A wide band centered at about 1.4 eV was observed with lower intensity than that of the excitonic lines. This emission band, due to its distinctive profile, is ascribable to the typical DAP transition related to the A-center of V_{Cd}-III_{Cd} complex as already observed in CdTe and CZT for Al, Ga, and In. This center is well distinguishable from other centers due to its very broad emission band which is strongly phonon coupled, at an energy that is far below the band-gap energy. In this energy range, other attributions have been reported in the literature, as discussed below after careful analysis of the PL profile. It is possible that contributions from several other impurities overlap in this spectral region.

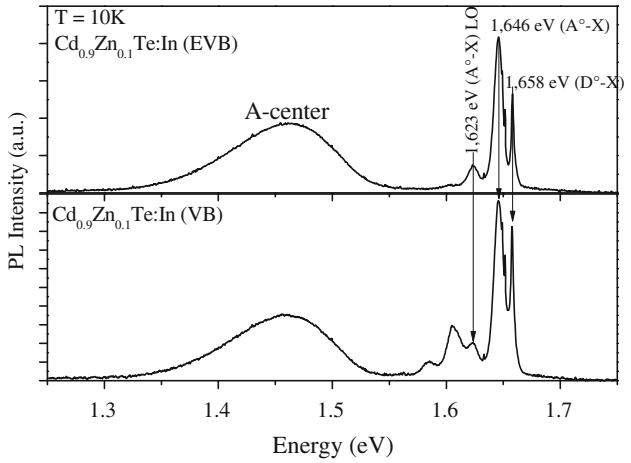

Fig. 1. Low-temperature PL spectra (10 K): (a) EVB sample of CZT:In and (b) VB sample of CZT:In.

Unfortunately, due to the greater crystalline disorder in the ternary alloy (CZT), no phonon replicas are visible and it is difficult to identify the energy of the zero-phonon line, as already reported by Stadler et al.[14] Further, due to the indium doping which is necessary for compensation and to obtain high-resistivity CZT, it is difficult to isolate indium and boron contributions. Indeed, similar PL contributions from elements of the same chemical group are to be expected.

No significant change has been evidenced in comparison with VB samples grown without encapsulant (Fig. 1b) except for some small differences ascribable to variations in zinc concentration. Actually, the two samples were cut from two ingots in which the zinc and indium distributions and microscopic order are slightly different.

As known, the broad luminescence at 1.4 eV shows a well-resolved structure in CZT with extreme zinc content ($x = 0$ or $x = 1$).[7,16] In addition, since the band-gap difference between CdTe and CZT (10% Zn) is 62 meV at 300 K, any shift in the ionization energies of defects is expected to be relatively small. Thus, CdTe samples were grown by the encapsulated vertical Bridgman technique without doping to reveal the real contribution of boron to the PL spectra. Since doping in CdTe is not essential to achieve high-resistivity material, in this case any emission related to indium in PL measurements is removed. A typical low-temperature PL spectrum is shown in Fig. 2, where a wide, 1.4-eV band is clearly

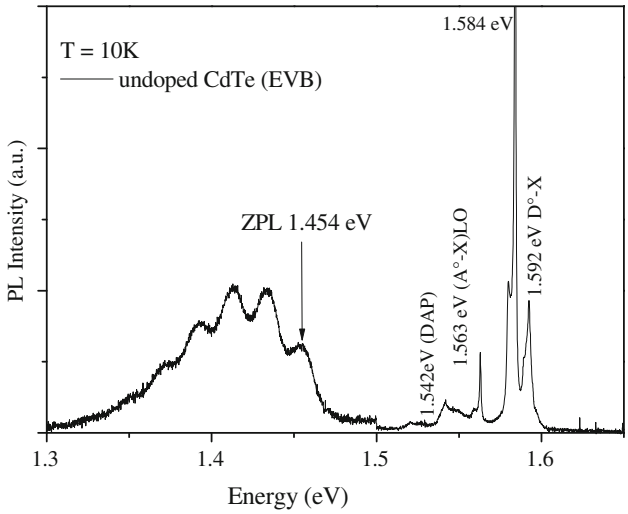

Fig. 2. Low-temperature PL spectra for undoped CdTe grown by EVB. For clarity, the A-center band in EVB sample was increased by a factor 2.5. The line at 1.584 eV was already observed in high-resistivity CdTe doped with group III elements.[17,18]

evident, and the phonon replicas are well visible. The absence of In dopant and the low concentration of other impurities belonging to group III or VII together with the profile of this emission band, which is typical of A-centers, suggest the involvement of boron in this donor–vacancy complex. In the literature, A-center involving boron has not been reported, whereas an Al-related A-center was measured in ZnTe.[19] Furthermore, comparison with the In-related A-center from the literature (see, for example, Ref. 14) shows distinctive features with respect to our undoped EVB sample, the relative intensities of the phonon replicas and the Huang–Rhys factor being the most evident differences.

Chattopadhyay et al.[20] showed PL spectra for undoped CdTe with boron contamination from a BN-coated ampoule, but the impurity level of indium (1000 ppba) does not exclude the attribution of the 1.4-eV band to both boron and/or indium. In our case it is noteworthy that the indium impurity concentration is lower than the detection limit of the GDMS technique.

The zero-phonon line (ZPL) at 1.454 eV is associated with a few phonon replicas, which are separated by approximately 21 meV. The appearance of multiple phonon replicas may be an indication of long-range crystalline order in the crystal, and it certainly indicates the strength of the coupling between the localized electrons (or holes) and the lattice. Normally, this coupling is of low or moderate strength for excitonic and impurity level to band recombinations and is stronger for donor–acceptor pair (DAP) emissions.

The intensity of the set of phonon replicas is described by the Poisson distribution. Fitting of the data using the Huang–Rhys formula reported in Ref. 21 gives a Huang–Rhys coupling parameter of $S = 3.1$. When the S factor is large, the zero-phonon emission peak will be low in amplitude in comparison with higher-order peaks, as evidenced in Fig. 2.

Table II. Activation energy and Huang–Rhys factor for some dopant elements of groups III and VII in CdTe (literature data from Ref. 14)

Donor	Group	E_B	S
F	VII	116	3.2
Cl	VII	125	2.2
Br	VII	119	2.6
I	VII	128	1.5
Ga	III	131	1.7
In	III	142	1.8
B (this work)	III	138	3.1

The activation energy E_B, measured as the difference between the band edge and the reduced value of the ZPL binding energy for the donor (14 meV as in Stadler et al.[14]), is 137 meV. A value of 142 meV was obtained for CdTe:In with a Huang–Rhys factor of 1.8 (Table II), far from the value obtained for boron.

It is immediately plain (Table II) that PL measurements on CdTe samples grown with encapsulant are characterized by an activation energy that is typical of elements belonging to group III, while the Huang–Rhys factor is similar to those for light elements, in particular fluorine, whose atomic weight is very close to that of boron.

Other relevant contributions to the 1.4-eV PL band in CdTe have been ascribed to impurities such as copper, silver, and gold. The values of activation energy and Huang–Rhys factor ($E_B = 263$ meV and $S = 3.1$ for CdTe:Au,[22] $E_B = 146$ meV and $S = 1.5$ for CdTe:Cu,[23] $E_B = 108$ meV and S = 0.9 for CdTe:Ag[23]) do not match with values obtained from our PL spectra. However, the concentration of these impurities in our crystals is negligible, and we can exclude their effects can be detected on the PL spectra.

The PL intensity mapping over the whole area of a slice cut along the axis of a CZT:In ingot grown by EVB for the energy band at 1.4 eV is shown in Fig. 3 (top). A similar result was obtained for CZT grown without encapsulant. This suggests that the 1.4-eV energy band is mostly generated by a defect related to indium.

The first-to-freeze material is at the bottom of the picture. Along the axis (bottom to top), the intensity generally increases along the crystal growth direction. This is due to the fact that the segregation coefficient of indium is lower than 1 (around 0.3), so that indium concentration is expected to increase during growth.[24] Actually, at the very beginning of growth, a decrease in the intensity of the 1.4-eV band is observed. This effect should be related to the anomalous segregation behavior which was registered at the beginning of growth, as also seen by other authors.[25] Along the radius, the indium distribution follows the convex shape of the growth interface (the center is on the right).[26]

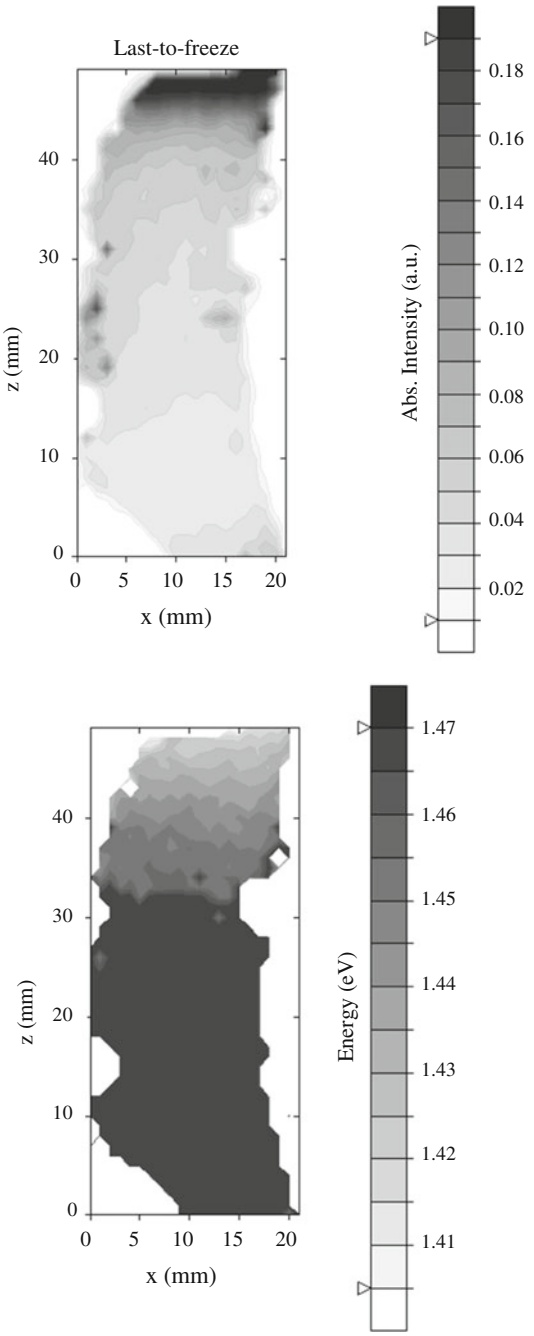

Fig. 3. PL mapping along the ingot axis: intensity of the 1.4-eV band (top), and energy of maximum intensity of the 1.4-eV band (bottom).

Figure 3 (bottom) shows the energy distribution of the maximum intensity of the 1.4-eV band along the slice.

In the main part of the crystal, the energy with maximum intensity is clearly fixed at about 1.47 eV, confirming an almost uniform distribution of the elements involved in the A-center. Towards the end of the crystal, the energy of the band maximum lowers, which can be attributed to the fact that, as the distribution coefficient of zinc in CdTe is higher than 1 (about 1.35), the zinc concentration is lower at the end of the crystal. This fact causes a reduction of the band-gap energy and, thus, a decrease in the energy of the maximum of the 1.4-eV band.

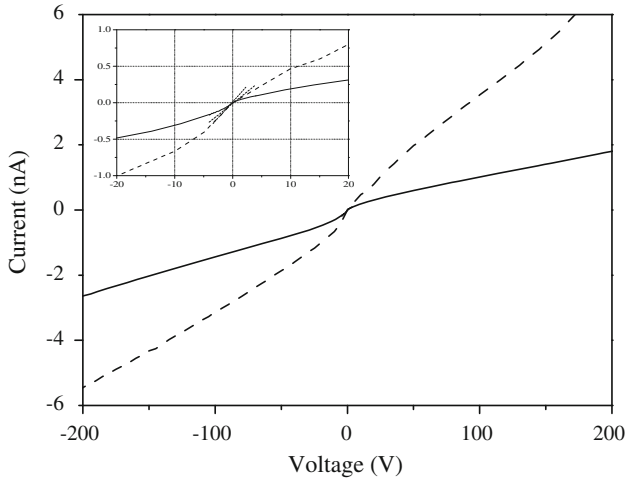

Fig. 4. *I–V* curves for EVB (solid line) and VB (dashed line) CZT samples. The inset shows an enlargement at low voltages.

Electrical Measurements on CZT Samples

To test our material resistivity, van der Pauw measurements were carried out. However, it was not possible to make reliable measurements using this technique due to the effects of strong surface conduction. Current–voltage (*I–V*) characteristics of samples, prepared as described in the "Experimental Procedures" section, were studied, and the results showed that surface currents can be reduced significantly through use of both a guard ring and careful passivation of the lateral surfaces of the samples. Typical *I–V* curves are shown in Fig. 4 for EVB (solid line) and VB (dashed line) CZT samples. The characteristic trend can be explained as that of two back-to-back diodes realized on a high-resistivity material, and the resistivity of the bulk material can be calculated from the slope of the *I–V* curve at low voltage ($|V| < 1$ V, inset in Fig. 4) as reported by Prokesch and Szees;[27] otherwise, the resistivity could be erroneously deduced at high bias, resulting in a value a few times higher. Resistivities of about 10^{10} Ω cm were observed for both EVB [$(3.4 \pm 0.2) \times 10^{10}$ Ω cm] and VB [$(3.3 \pm 0.2) \times 10^{10}$ Ω cm] samples along the whole ingots. The high resistivity can be attributed to the indium doping, even if a possible contribution of iron contamination to the compensation cannot be excluded.

The steady-state photocurrent (PC) technique provides some interesting information about transport parameters such as the mobility–lifetime product $\mu\tau$ and other terms related to surface recombination, playing a role complementary to high-energy photon spectroscopy. Due to its lower penetration depth, PC provides an evaluation of the

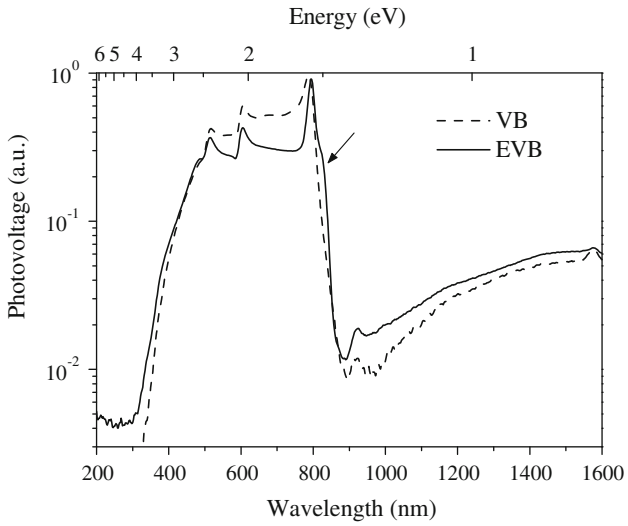

Fig. 5. Illuminated *I–V* curves for 786 nm (curves normalized to the saturation current at high electric field).

surface quality of samples. Photocurrent spectral analysis adds the ability to investigate the nature of bulk trap levels, surface centers, contact layer defects, and the distribution of the electric field in the sample volume.

Photovoltage spectra for EVB samples are shown in Fig. 5 on a semilogarithmic plot for negative bias (−200 V) at the same incoming photon flux. The investigated energy interval can be divided into three regions: (1) a high-energy region (200 nm to 700 nm) in which the contributions from the surface oxides can be found,[28–32] (2) the CZT band-edge region around 800 nm, and (3) a low-energy region (830 nm to 1600 nm) characterized by shallow and deep levels of bulk material or other unwanted complexes. In particular, a shoulder on the right side of the band edge, centered at about 830 nm, and a localized weak peak at about 922 nm probably due to CdO indirect gap transition, were evidenced.

The shoulder could be related to the well-known A-center, a complex which is formed by a Cd vacancy and In_{Cd}, and perhaps to other shallow centers. Focusing attention on this third region of spectra, it is possible to highlight a difference between the samples with and without boron encapsulation: the sample grown by EVB shows a larger photovoltage in the range between 800 and 870 nm. This result seems to suggest a different involvement of the A-center in the mechanisms which are responsible for the photostimulated current. This may be due to a different concentration of A-centers or a different interaction with the lattice. The high value of the *S* factor for boron involved in the A-center in undoped CdTe could explain this result. Careful studies are in progress to cast light on this topic.

Finally, the $\mu\tau$ product, which indicates good spectroscopic features, was evaluated by photoilluminated *I–V* curves as indicated by Many.[13] The samples were excited by photons near the band-gap at flux values suitable to minimize surface effects, then the curves were fitted using Many's equation. The fitting procedure was performed by least-squares method, and the experimental error for the current values is about 1% of full scale. The values obtained ($\mu\tau_e = 1.3 \times 10^{-3}$ cm^2 V^{-1} and $\mu\tau_h = 5.0 \times 10^{-5}$ cm^2 V^{-1}) for the EVB samples are similar to those obtained for VB samples, supporting the hypothesis that boron is not detrimental to device performance. To check this statement, the spectroscopic properties of samples were evaluated by x-ray spectroscopy.

The material was then directly tested as a detector in planar geometry; the results are not reported herein, as they have already been presented in Ref. 31 by the same authors. The measured resolution at the 59.5-keV line of the ^{241}Am source is 4.9% and at the 88-keV line of the cadmium source is 3.7%. Moreover, many low-energy lines of the two spectra are clearly resolved, such as the CdTe escape peaks, suggesting that the detectors have good transport properties and that the carrier collection efficiency is high, as required to achieve a fully active detector.

Measurement of the $\mu\tau$ product was carried out to characterize the charge transport properties of the samples. Detectors were irradiated by the 22-keV line of a ^{109}Cd source from the cathode side, and energy spectra were recorded at different bias voltages in the same geometry as for PC. The photopeak centroids at 22 keV as a function of bias were fitted using the simplified Hecht relation.[32] The value obtained was $\mu\tau_e = (1.9 \pm 0.2) \times 10^{-3}$cm^2 V^{-1}, in agreement with the results obtained by PC measurements.[31]

CONCLUSIONS

Formation of A-centers with boron as a donor was evidenced in undoped CdTe crystals grown by the boron-encapsulated vertical Bridgman technique by means of low-temperature PL measurements. A wide, broad band centered at 1.4 eV was attributed to the B_{II}-V_{Cd} complex, with activation energy very close to values that are typical of group III donors (such as In and Ga) and Huang–Rhys coupling factor near the value for fluorine, which is as light as boron. A contribution by indium was excluded because CdTe is undoped and the concentration of other impurities, giving PL bands in the same spectral region, is too low to be detected.

We expected similar behavior for boron in CZT, but in this case we were not able to distinguish its luminescence contribution. The low crystalline order of the ternary alloy prevented us from resolving the phonon replicas. In addition, indium doping hides the presence of boron in PL measurements.

Electrical features of CZT grown by EVB are comparable to those of VB CZT. For these reasons, the new EVB method has proved to be a good

candidate for production of large quantities of CZT, since boron contamination during growth is one order of magnitude lower than the concentration of the dopant introduced in CZT to obtain high resistivity.

The new technique shows at least four important technological advantages: (1) sticking of the crystals to the quartz walls is prevented, (2) the stress generated in the crystal by the crucible during growth is avoided, (3) the stress generated in the crystal by the crucible during the cooling procedure is prevented, and (4) the boron oxide layer can work as a barrier against migration of impurities from the crucible to the crystal. As a consequence, crystals with an extremely low number of dislocations and very high quality have been obtained.

ACKNOWLEDGEMENTS

Authors are grateful to Dr. E. Caroli, Dr. N. Auricchio, and Dr. G. Ventura for helpful discussion and to Mr. A. Donati (INAF-IASF Bologna-Italy) for technical support. This work was partially supported by Agenzia Spaziale Italiana (ASI) under Program No. I/073/06/0 "Rivelatori spettroscopici X and γ in CZT."

REFERENCES

1. T.E. Schlesinger, J.E. Toney, H. Yoon, E.Y. Lee, B.A. Brunett, L. Francks, and R.B. James, *Mater. Sci. Eng.* 32, 103 (2001).
2. C. Szeles, S.E. Cameron, S.A. Soldner, J.O. Ndap, and M.D. Reed, *J. Electron. Mater.* 33, 742 (2004).
3. L.G. Casagrande, D.D. Marzio, M.B. Lee, D.J. Larson Jr, M. Dudley, and T. Fanning, *J. Cryst. Growth* 128, 576 (1993).
4. R. Shetty, R. Balasubramanian, and W.R. Wilcox, *J. Cryst. Growth* 100, 51 (1990).
5. M. Zha, A. Zappettini, D. Calestani, L. Marchini, L. Zanotti, and C. Paorici, *J. Cryst. Growth* 310, 2072 (2008).
6. A. Zappettini, M. Zha, M. Pavesi, and L. Zanotti, *J. Cryst. Growth* 307, 283 (2007).
7. D.M. Hofmann, P. Omling, H. Grimmeis, B.K. Meyer, K.W. Benz, and D. Sinerius, *Phys. Rev. B* 45, 6247 (1992).
8. G.W. Blackmore, S.J. Courtney, A. Royle, N. Shaw, and A.W. Vere, *J. Cryst. Growth* 85, 335 (1987).
9. E. Gombia, F. Bissoli, M. Zha, A. Zappettini, and L. Zanotti, *Phys. Stat. Sol. (c)* 0, 881 (2003).
10. A. Zappettini, T. Görög, M. Zha, L. Zanotti, G. Zuccalli, and C. Paorici, *J. Cryst. Growth* 214–215, 14 (2000).
11. M. Zha, F. Bissoli, A. Zappettini, G. Zuccalli, L. Zanotti, and C. Paorici, *J. Cryst. Growth* 237–239, 1720 (2002).
12. L. Marchini, A. Zappettini, E. Gombia, R. Mosca, M. Lanata, and M. Pavesi, *IEEE Trans. Nucl. Sci.* 56, 1823 (2009).
13. A. Many, *Phys. Chern. Solids* 26, 575 (1965).
14. W. Stadler, D.M. Hofmann, H.C. Alt, T. Muschik, B.K. Meyer, E. Weigel, G. Müller-Vogt, M. Salk, E. Rupp, and K.W. Benz, *Phys. Rev. B* 51, 10619 (1995).
15. C.H. Park and D.J. Chadi, *Phys. Rev. B* 52, 11884 (1995).
16. W. Palosz, K. Grasza, P.R. Boyd, Y. Cui, G. Wright, U.N. Roy, and A. Burger, *J. Electron. Mater.* 32, 747 (2003).
17. J.M. Wrobel, J.J. Dubowski, and P. Becla, *J. Vac. Sci. Technol. A* 7, 338 (1989).
18. S. Seto, A. Tanaka, K. Suzuki, and M. Kawashima, *J. Cryst. Growth* 101, 430 (1990).
19. J. Bittebierre and R.T. Cox, *Phys. Rev. B* 34, 2360 (1986).
20. K. Chattopadhyay, S. Feth, H. Chen, A. Burger, and C.-H. Su, *J Cryst. Growth* 191, 377 (1998).
21. K. Huang and A. Rhys, *Proc. R. Soc. Lond. Ser. A* 204, 406 (1950).
22. E. Molva, J.L. Pautrat, K. Saminadayar, G. Milchberg, and N. Magnea, *Phys. Rev. B* 30, 3344 (1984).
23. J.P. Chamonal, E. Molva, and J.L. Pautrat, *Solid State Commun.* 43, 801 (1982).
24. M.G. Astles, Impurity doping in CdTe.*Narrow Gap Cadmium Based Compounds*, ed. P. Capper (London: INSPEC, IEE Publishing, 1994).
25. M. Muhlberg, P. Rudolph, C. Genzel, B. Wermke, and U. Becker, *J. Cryst. Growth* 101, 275 (1990).
26. L. Marchini, N. Zambelli, G. Piacentini, M. Zha, D. Calestani, E. Belas, and A. Zappettini, in press on *Nucl. Instrum. Methods Phys. Res.* Corrected Proof Available online 7 July 2010 http://www.sciencedirect.com/science/article/pii/S0168900210013239.
27. M. Prokesch and C. Szeles, *J. Appl. Phys.* 100, 014503 (2006).
28. A. Iribarren, E. Menéndez-Proupin, R. Castro-Rodríguez, V. Sosa, J.L. Peña, and F. Caballero-Briones, *J. Appl. Phys.* 86, 4688 (1999).
29. H. Tetsuka, Y.J. Shan, K. Tezuka, and H. Imoto, *Solid State Commun.* 137, 345 (2006).
30. A.A. Dakhel and F.Z. Henari, *Cryst. Res. Technol.* 38, 979 (2003).
31. A. Zappettini, M. Zha, L. Marchini, D. Calestani, R. Mosca, E. Gombia, L. Zanotti, M. Zanichelli, M. Pavesi, N. Auricchio, and E. Caroli, *Trans. Nucl. Sci.* 56, 1743 (2009).
32. K. Hecht, *Z Phys A* 77, 235 (1932).